

Parker, Andrew J. ORCID: <https://orcid.org/0000-0002-6851-6383> , Joyce, Malcolm J. and Boxall, Colin (2016) Radiometric detection of non-radioactive caesium flux using displaced naturally abundant potassium. *Journal of Radioanalytical and Nuclear Chemistry*, 307 (1). pp. 769-776.

Downloaded from: <http://insight.cumbria.ac.uk/id/eprint/2629/>

*Usage of any items from the University of Cumbria's institutional repository 'Insight' must conform to the following fair usage guidelines.*

Any item and its associated metadata held in the University of Cumbria's institutional repository Insight (unless stated otherwise on the metadata record) may be copied, displayed or performed, and stored in line with the JISC fair dealing guidelines (available [here](#)) for educational and not-for-profit activities

**provided that**

- the authors, title and full bibliographic details of the item are cited clearly when any part of the work is referred to verbally or in the written form
  - a hyperlink/URL to the original Insight record of that item is included in any citations of the work
- the content is not changed in any way
- all files required for usage of the item are kept together with the main item file.

**You may not**

- sell any part of an item
- refer to any part of an item without citation
- amend any item or contextualise it in a way that will impugn the creator's reputation
- remove or alter the copyright statement on an item.

The full policy can be found [here](#).

Alternatively contact the University of Cumbria Repository Editor by emailing [insight@cumbria.ac.uk](mailto:insight@cumbria.ac.uk).

# **Radiometric detection of non-radioactive caesium flux using displaced naturally abundant potassium**

Andrew J. Parker<sup>1</sup>, Malcolm J. Joyce<sup>2</sup>, Colin Boxall<sup>2</sup>

<sup>1</sup>*Department of Medical & Sports Sciences, University of Cumbria, Lancaster, LA1 3JD, UK*

<sup>2</sup>*Department of Engineering, Lancaster University, Lancaster, LA1 4YR, UK*

## **Abstract**

We report on a method that allows for the radiometric detection of non-radioactive caesium by the measurement of potassium ions displaced from an ion exchange barrier. Electrokinetic transport of  $K^+$  and  $Cs^+$  through concrete samples was measured using a bespoke scintillation detector to monitor electrolyte concentrations. Results show experimental ionic flux and diffusion parameters of non-active caesium ( $\sim 1 \times 10^{-5} \text{ mol m}^{-3}$ ) were consistent with those recorded for potassium and also with values reported in relevant literature. This work demonstrates a novel concept that can be applied to proof-of-concept studies that help develop the next generation of nuclear decommissioning technologies.

## **Keywords**

Nuclear decommissioning, gamma spectroscopy, caesium 137, non-hazardous radioactive tracer, ion exchange.

## Introduction

Radioactive fission products produced in the nuclear fuel cycle are perhaps the single largest contributor to the challenge of managing nuclear waste and the safe decommissioning of nuclear facilities. Of all the fission products  $^{137}\text{Cs}$  is the isotope of most interest due to its radiological and chemical properties; caesium has high solubility over a wide pH range rendering it extremely mobile in the environment;  $^{137}\text{Cs}$  has a high specific activity and decaying through a high-energy  $\gamma$ -ray emission.

These properties, as well as creating the safety and environmental issues in the real-world, also contribute to the difficulty of using the isotope in laboratory and bench-top scale experimental studies. Such studies are necessary for researching and developing the next generation of technologies needed to combat the issues faced in the clean-up of the nuclear legacy.

This short communication presents a method of detecting the electrokinetic transport of non-active caesium, using radiometric equipment, through concrete samples based on work previously carried out [1]. The purpose of the work is to demonstrate that the study of new decommissioning techniques (e.g. electrokinetic remediation) can be achieved using the same measurement technologies and contaminants without any of the safety issues. To accomplish this, the method utilises high-sensitivity gamma spectroscopy, ion exchange, and naturally abundant potassium.

## Methods and Materials

### *Experimental Setup*

The electrokinetic experiments were carried out using a radioanalytical phantom, shown in Figure 1. The analytical phantom used was similar to the one described in previous work [2], as such only a concise description of the set-up is given in this work. Concrete samples were sealed into a polypropylene pipe connecting two electrolyte compartments: the volume of each compartment was 1.04 litres. The external DC necessary for the generation of electrokinetic transport was provided by an EL302T power supply (Thrulby Thandar Instruments), set to an applied voltage of 60 V. To prevent electrolyte heating, and unwanted electroosmotic flow, the current was limited to a maximum of 35 mA. The power supply was connected to a mild steel reinforcement bar cathode, and a platinised titanium mesh anode. The anode and cathode were both mounted 50 mm from the surface of the concrete samples within the respective compartments. Two additional platinum electrodes were placed at the anodic and cathodic facing surfaces of the concrete sample to measure the potential difference across the length of the samples.

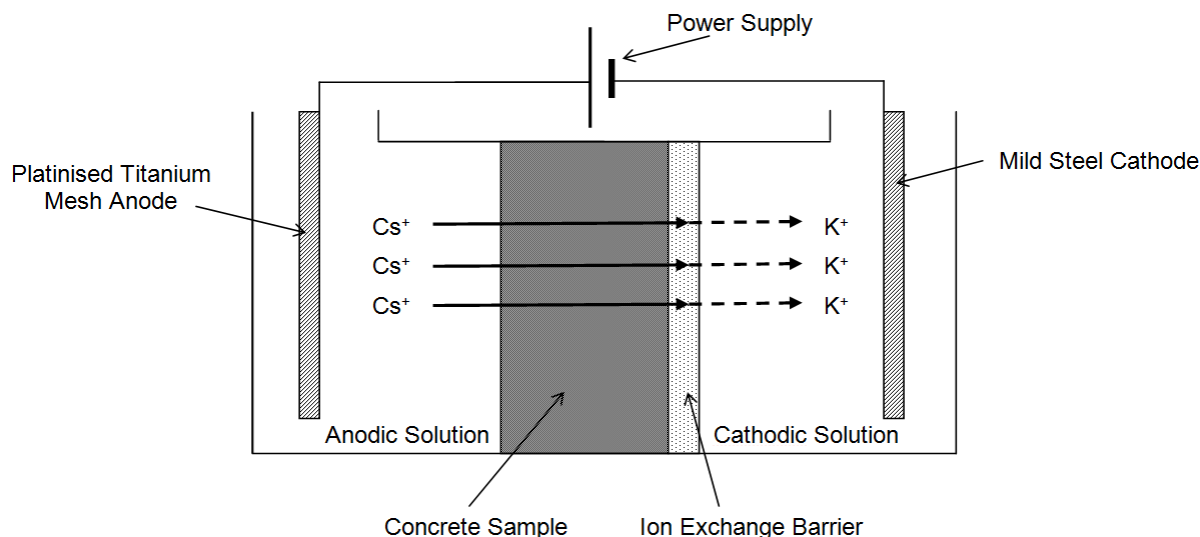


Figure 1. Sketch of the electrochemical fuel pond phantom showing the location of the concrete sample and the adjacent ion exchange barrier.

### *Experimental Regime*

The experiments were conducted in two phases; firstly the radiometric measurement of the transport rates of potassium ions driven by the external electric field was conducted. This allowed for the determination of ionic flux through the samples without the complication of the ion exchange displacement barrier. The second phase was the radiometric measurement of non-active caesium ion transport under the influence of the external electric field.

The ion exchange barrier consisted of a 30 gram Lewatit Monoplus S 108 KR ion exchange resin bed, formed between two ion-permeable membranes mounted in a polypropylene ring. The barrier was placed immediately adjacent to the cathodic-facing surface of the concrete samples within the connecting tube between the two electrode compartments. The ion exchange resin was converted from its manufacturer-shipped  $H^+$  form to a  $K^+$  form by washing the resin in a  $500\text{ g l}^{-1}$  solution of KCl for four hours. Based on the manufacturers information the barrier is estimated to have a total exchangeable capacity of 75 mmol [3].

The mechanism for the ion exchange barrier is shown in Equation (1); caesium ions migrating through the concrete, under the influence of the electric field, pass into the ion exchange barrier where they exchange with potassium ions. The potassium ions are also influenced by the electric field and migrate into the catholyte where they can be detected. For the potassium transport studies the ion exchange barrier was removed from the electrochemical phantom.



For the two phases of experiments the starting anolyte consisted of KCl and CsCl solutions with concentrations of 396 and 70 mol m<sup>-3</sup>, respectively. The concentration of KCl was chosen to maximise the chances of radiometric detection and the concentration of CsCl was based on the exchangeable capacity of the ion exchange barrier. In addition to the KCl or CsCl, the electrolyte in each compartment contained a 100 mol m<sup>-3</sup> NaOH solution to match the highly alkaline cementitious pore solutions and to prevent the corrosion of the anode.

### *Concrete*

The concrete samples used throughout this work were mixed with a 3:2:1 ratio (coarse pebble aggregate, siliceous sand, and Ordinary Portland Cement), in accordance with European Standard E206-1. The mixed concrete was poured into cylindrical polypropylene moulds, 150 mm long with an inner diameter of 105 mm, and left to cure for 28 days. At the end of the curing period the cylinders were cut into smaller thickness sections (25, 35, 65 mm) using a diamond toothed circular saw to ensure a smooth surface. The thickness of the concrete samples was chosen based on comparable studies in literature and to provide a range of widths which the ionic flux could be measured against.

## *Transport Detection and Sampling*

The ionic transport through the concrete samples was assessed radiometrically using a bespoke NaI(Tl) well-type scintillation counter [4]. Following the start of the experiments 40 ml aliquots of the catholyte were sampled on a daily basis. The aliquots were then placed in the detector setup, shown in Figure 2. Samples were counted over a 4 hour period. This period was chosen as it gave enough time to achieve good counting statistics whilst remaining a small percentage of the overall experimental duration.



*Figure 2. The NaI(Tl) well counter used in this work. The lead blocks have been removed from the top of the instrument to provide a better view of the detector.*

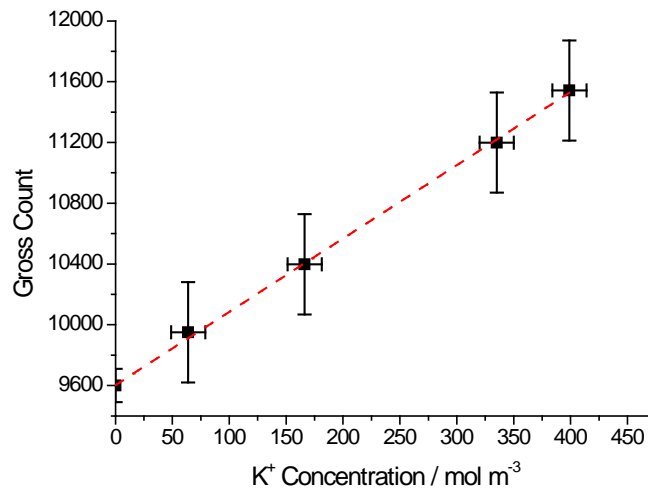


Figure 3. The relationship between the gross count and potassium concentration of a 40ml KCl sample, where  $y = mx + c$ ,  $m = 4.74 \pm 0.1$ ,  $c = 9609 \pm 28.2$ ,  $R^2 = 0.9994$ .

Calibration experiments were conducted by detecting 40 ml sample KCl solutions of known concentration (between 0-400 mol m<sup>-3</sup>) for four hours in the detection setup. The results of the calibration are shown in Figure 3. Using the calibration relationship derived from Figure 3 it is possible to convert gross count data from the analysis of cathode solutions to solution concentrations. Caesium concentration values are determined based on the uni-univalent ion exchange mechanism described by Equation (1).

## Results and Discussion

### *Potassium Transport*

The effect that the application of the electric field had on the rate of K<sup>+</sup> transport through the concrete samples can be seen in Figure 4.



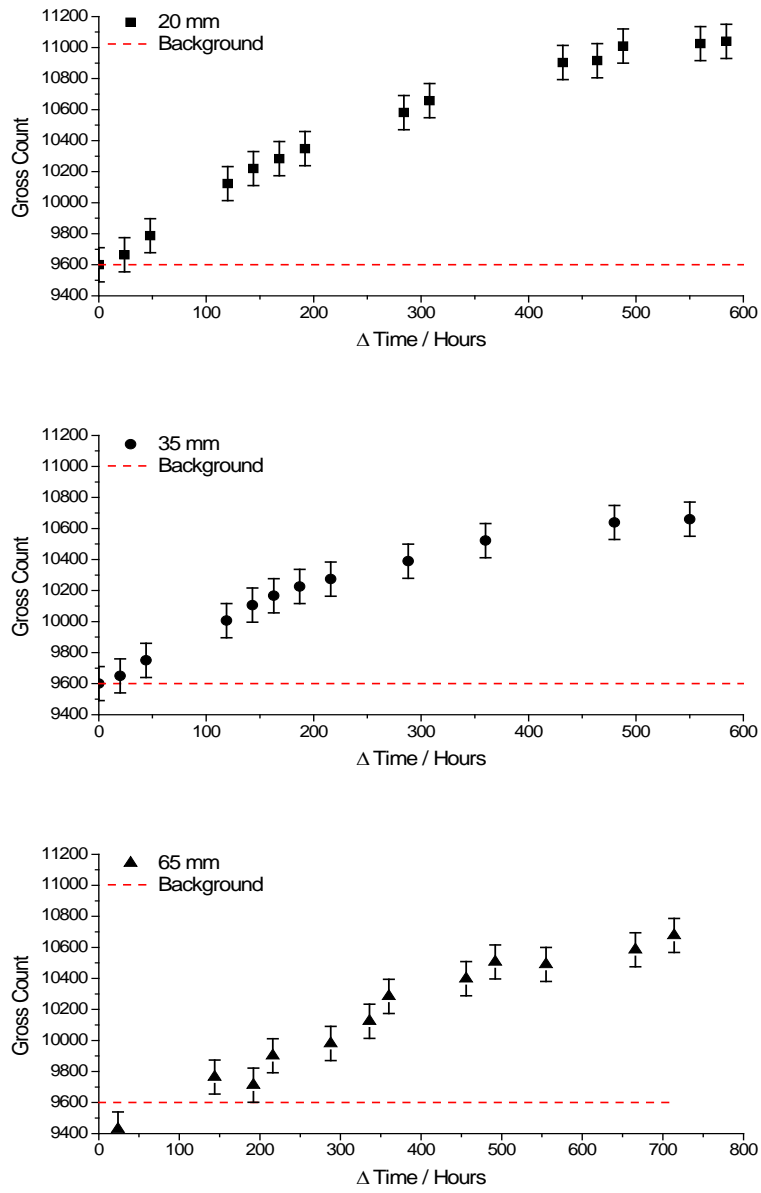


Figure 4. Change in net count from 40 ml catholyte samples taken to determine  $K^+$  transport across 20, 35, and 65 mm concrete samples with a 60 V 35 mA electric field applied.

Using the experimental data of Figure 4, the ionic flux and diffusion coefficient were calculated for each sample using a simplified Nernst-Planck equation derived by Andrade [5]:

$$D_{SNP} = \frac{JRTl}{zFcE} \quad (2)$$

where  $z$  is the valence of the ionic species,  $c$  is the initial anodic concentration ( $\text{mol m}^{-3}$ ),  $F$  the Faraday constant ( $96484.6 \text{ C mol}^{-1}$ ),  $R$  the ideal gas constant ( $8.314 \text{ J mol}^{-1} \text{ K}$ ),  $E$  the electric potential (V),  $l$  the thickness of the concrete sample (m), and  $J$  is the steady state ionic flux ( $\text{mol m}^{-2} \text{ s}^{-1}$ ).  $J$  is determined using the following equation [5]:

$$J = \frac{\Delta cV}{S\Delta t} \quad (3)$$

where  $\Delta c$  is the change in cathodic concentration ( $\text{mol m}^{-3}$ ) over the time interval  $\Delta t$  (s),  $V$  is the cathodic volume ( $\text{m}^3$ ) and  $S$  is the surface area of the concrete exposed for ionic transport ( $\text{m}^2$ ).

Given the requirement that the system should be in a steady-state of flux for the correct application of Equations (2 and (3, only data points recorded during the 200 hours sampling time immediately following the point of detectable potassium breakthrough into the catholyte – subsequently referred to as the point of ionic breakthrough (PIB) – were used in the calculation of  $J$  and  $D_{SNP}$ . In this range, gross count shows a linear or near linear dependence on time, indicating accordance with the Andrade assumptions above [5]. Shown in Figure 5 are the data points recorded during the pre-PIB period and for the 200 hour period after the observed PIB. Also shown in the figure are the linear steady-state regression fits of the post-PIB data and their associated error. The slope of the straight line derived from the regression analysis provides the basis for the calculation of ionic flux and the simplified Nernst-Planck theory-derived diffusion coefficient. The calculated values, and the associated error, for the different concrete samples are shown in Table 1.

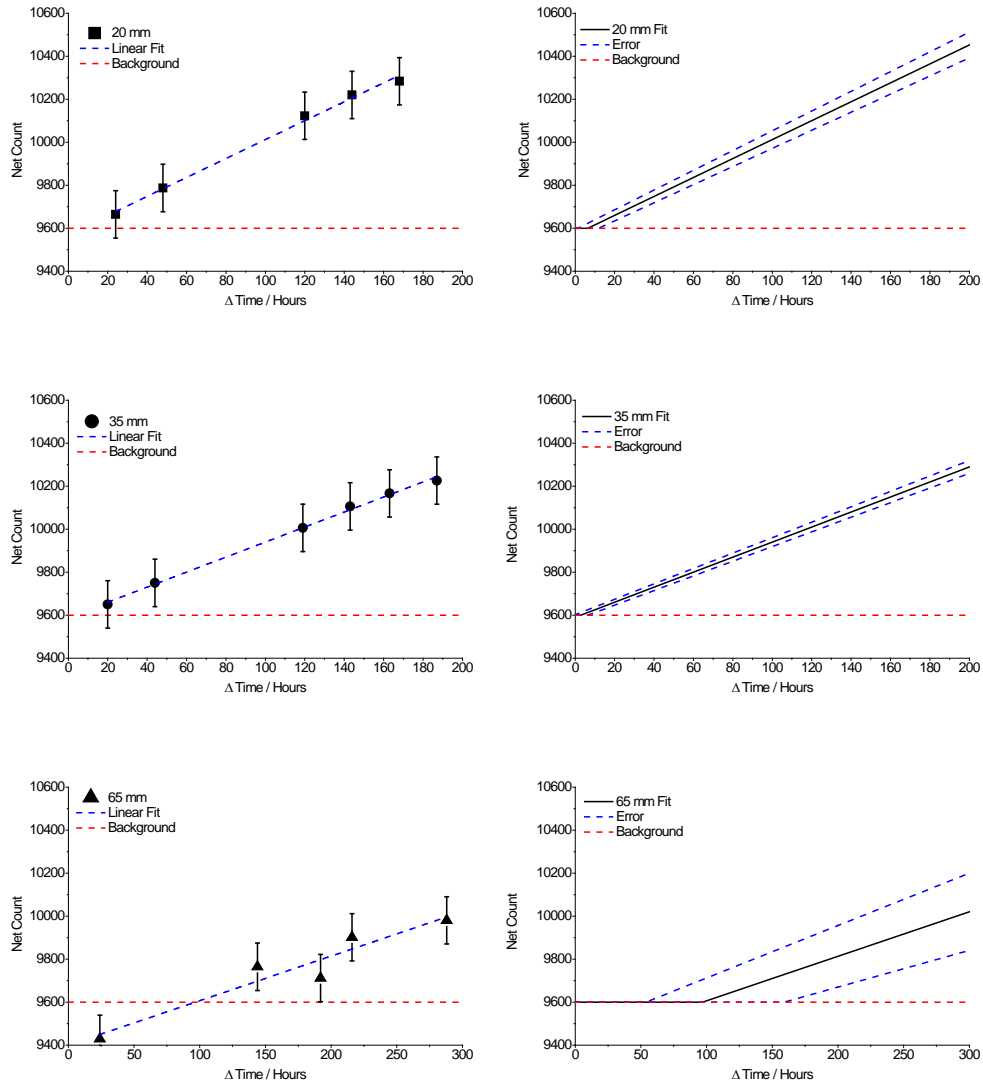


Figure 5. Change in gross count as a function of experimental time and the steady-state linear regression of data recorded after the point of ionic breakthrough, indicative of the  $K^+$  flux through concrete samples.

Table 1. The derived steady-state ionic flux values and Simplified-Nernst-Planck diffusion coefficient. Values taken from electrokinetic transport experiments using  $70 \text{ mol m}^{-3}$  CsCl solutions, with other experimental parameters shown in the table.

| Ion          | Anolyte Conc. ( $\text{mol m}^{-3}$ ) | Sample Thickness (mm) | Applied Potential (V) | Measured Potential (V) | Current (mA) | $J$ ( $\text{mol m}^{-2} \text{ s}^{-1}$ ) | $D_{\text{SNP}}$ ( $\text{mol m}^{-2}$ ) |
|--------------|---------------------------------------|-----------------------|-----------------------|------------------------|--------------|--|--|
| $\text{K}^+$ | 396                                   | 20                    | 60.1                  | 59.3                   | 35           | $2.71 (\pm 0.18) \times 10^{-5}$           | $5.81 (\pm 0.38) \times 10^{-13}$        |
|              |                                       | 35                    | 60.1                  | 58.9                   | 35           | $2.15 (\pm 0.38) \times 10^{-5}$           | $8.07 (\pm 0.39) \times 10^{-13}$        |
|              |                                       | 65                    | 60.1                  | 59.2                   | 35           | $5.65 (\pm 0.76) \times 10^{-6}$           | $3.93 (\pm 0.76) \times 10^{-13}$        |

The consistency of these results, relative to both each other and the literature, is demonstrated by the derived simplified-Nernst-Planck diffusion coefficients ( $D_{\text{SNP}}$ ) for electrokinetic transport experiments. All  $D_{\text{SNP}}$  values for  $\text{K}^+$  reported in Table 1 are in the same order of magnitude,  $1 \times 10^{-13} \text{ mol m}^{-2}$ . There is a slight variation in the values, outside of the calculated uncertainty ( $\pm 0.38 - 0.76 \times 10^{-13} \text{ mol m}^{-2}$ ). This, however, is consistent with the findings of Castellote *et al.* and Andrade *et al.* who observed wider variations, by an order of magnitude, in calculated electromigration diffusion coefficients through concrete samples with nominally identical compositions [6], [7]. Observed differences in diffusion coefficients, within this study and the work of Andrade *et al.*, are likely to be a result of local variations in the composition of the concrete samples [6]. The individual compositions (i.e. coarse aggregate, sand, cement, water ratio) will still vary between the concrete samples used in this work, despite being cut from the same larger concrete cylinder.

Concerns relating to the concrete composition variation aside, the observed  $D_{\text{SNP}}$  values for  $\text{K}^+$  are broadly consistent with those reported by Andrade *et al.* and Frizon *et al.* for the single valence elements;  $\text{Cl}^-$  and  $\text{Cs}^+$  respectively [6], [8], [9]. The experimental setups employed in the current study, the work of Frizon *et al.*, and to a lesser extent Andrade *et al.*, are all comparatively similar. The transport study performed by Frizon *et al.* is the closest in

design to this work where quantitative values are also defined. In the work by Frizon *et al.* a  $D_{\text{SNP}}$  of  $7.5 \times 10^{-12} \text{ mol m}^{-2}$  was observed for an initial analyte concentration of  $100 \text{ mol m}^{-3}$  [8]. Thus, the relative similarity of  $D_{\text{SNP}}$  with values obtained for  $\text{Cl}^-$ ,  $\text{K}^+$ , and  $\text{Cs}^+$  within these works provides support to the idea of using  $^{40}\text{K}$  as a radiological surrogate for  $^{137}\text{Cs}$ . Furthermore, the ionic transport results have shown that the radiological phantom provides a sound experimental design for studying the decontamination of active samples.

### *Caesium Transport*

The effect that the application of the electric field had on the rate of  $\text{Cs}^+$  transport through the concrete samples can be seen in Figure 6.

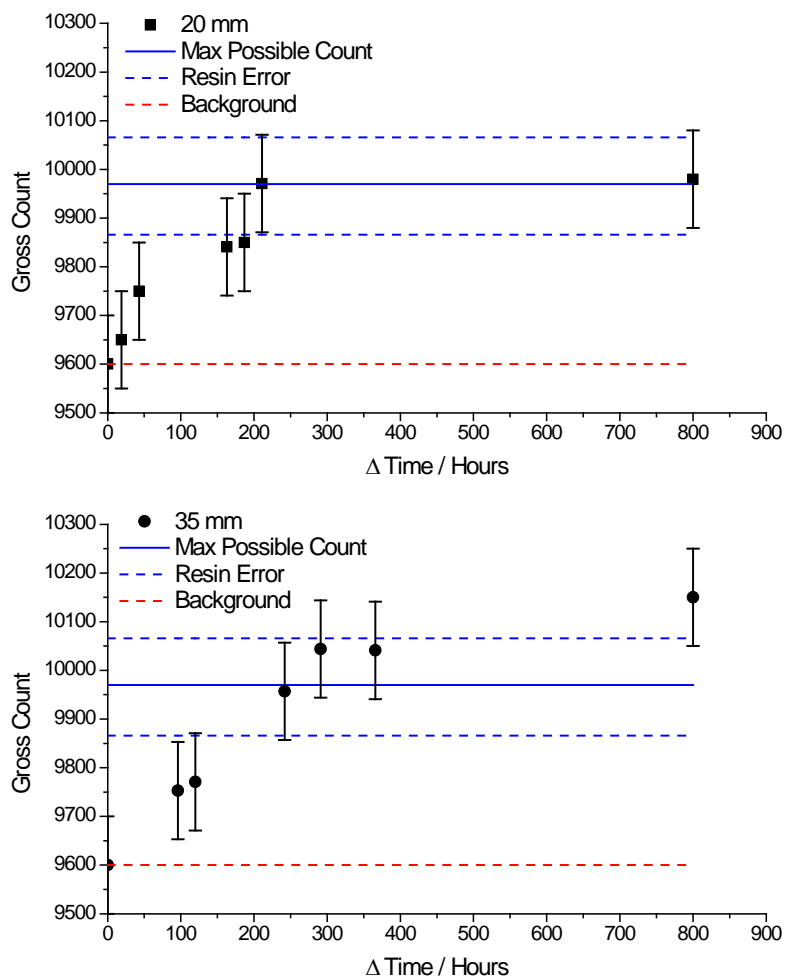


Figure 6. Change in gross count detected in catholyte as a result of  $K^+$  displacement from the receiving ion exchange resin by electro-migrating  $Cs^+$ . In each figure, the horizontal blue line represents the catholyte count that would be expected if all  $K^+$  were to be displaced from the receiving resin into the cathode chamber.

In Figure 6 the solid blue lines indicate the maximum count expected should the total mass of  $K^+$  initially loaded on the ion exchange barrier be exchanged with the migrating caesium and enter the catholyte. It can be seen that for both the 20 and 35 mm sample a plateau on the gross count is reached when the experiment is ended at approximately 800 hours.

Furthermore, in both cases it appears that the maximum amount of potassium has been exchanged from the resin with the migrating caesium.

Like the  $K^+$  transport study the simplified Nernst-Plank approach was used to evaluate the flux of ionic transport. Using the same steady-state assumption, only data points from the first 200 hours after the point of ionic breakthrough (PIB) were used. Shown in Figure 7 are the data points for the 200 hour period after the observed PIB. Also shown in the figure are the linear steady-state regression fits of the post-PIB data and their associated error. Again, the slope of the regression analysis provides the basis for the calculation of the flux of ionic transport and the simplified Nernst-Plank theory-derived diffusion coefficient, Equations (2 and (3. The calculated values, and the associated error, for the 20 and 35 mm concrete samples are shown in Table 2.

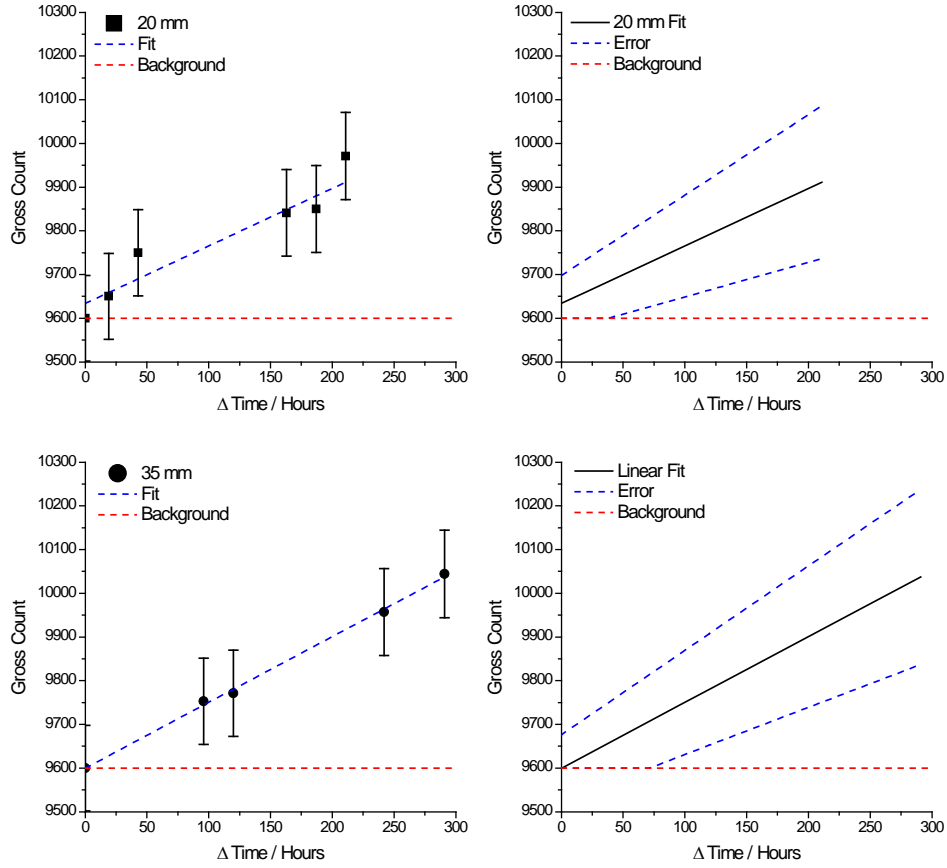


Figure 7. Steady State displaced  $K^+$  flux as a result of  $Cs^+$  migration through the samples as a function of total experiment time, and the linear regression showing the time of ionic breakthrough.

Not shown in Table 2 are the associated uncertainties. For  $Cs^+$  transport experiments the calculated error, for both  $J$  and  $D_{SNP}$ , are in the region of two orders of magnitude greater than the derived values. Given this high degree of uncertainty, conclusions are difficult to implicitly state however there is an apparent consistency with  $D_{SNP}$  values for  $Cs^+$  in literature. Frizon *et al.* recorded a  $D_{SNP}$  for  $Cs^+$  of  $7.5 \times 10^{-12} \text{ m}^2 \text{ s}^{-1}$  when electrokinetically transported through an 18 mm thick concrete sample [8].



Table 2. The derived steady-state ionic flux values and Simplified-Nernst-Planck diffusion coefficient. Values taken from electrokinetic transport experiments using  $70 \text{ mol m}^{-3}$  CsCl solutions, with other experimental parameters shown in the table.

| Ion             | Anolyte Conc. ( $\text{mol m}^{-3}$ ) | Sample Thickness (mm) | Applied Potential (V) | Measured Potential (V) | Current (mA) | $J$ ( $\text{mol m}^{-2} \text{ s}^{-1}$ ) | $D_{\text{SNP}}$ ( $\text{mol m}^{-2}$ ) |
|-----------------|---------------------------------------|-----------------------|-----------------------|------------------------|--------------|--|--|
| Cs <sup>+</sup> | 71                                    | 20                    | 60.1                  | 59.2                   | 35           | $8.90 \times 10^{-6}$                      | $1.09 \times 10^{-12}$                   |
|                 |                                       | 35                    | 60.1                  | 58.8                   | 35           | $1.02 \times 10^{-5}$                      | $2.18 \times 10^{-12}$                   |

Given the difference in the starting anolyte concentrations between the K<sup>+</sup> and Cs<sup>+</sup> trials, the ionic flux and  $D_{\text{SNP}}$  values for the Cs<sup>+</sup> transport experiments appear similar to those observed in the K<sup>+</sup> electromigration study. However, definite comparisons between the two studies and consequent conclusions cannot be made due to the magnitude of the calculated uncertainty in the final  $J$  and  $D_{\text{SNP}}$  values. The calculated ionic flux and diffusion in the K<sup>+</sup> study produced coefficient of variation (CoV) values in the range (0.066-0.177), where CoV is a normalised measure of dispersion [10]. Using the same measure of dispersion, CoV values for the non-active Cs<sup>+</sup> study were 5153 and 4713 for the 20 and 35 mm samples respectively. Such a large dispersion, in the case of the Cs<sup>+</sup> study, puts the calculated values for  $J$  and  $D_{\text{SNP}}$  on a much less sound statistical footing.

The source of this uncertainty is a compound of two experimental factors. Firstly, there is significantly less radiological content available for detection in the system. The total activity present in the non-active Cs<sup>+</sup> study was over five times less than the total activity in the K<sup>+</sup> study, ~92 Bq compared to ~492 Bq. The lower activity results in a decrease in the quality of counting statistics when using the same radiometric counting regime, i.e. 2 hour counts.

Secondly, taking into account the reduction in quality of counting statistics, the majority of the statistical uncertainty arises from the modification to the experimental setup necessary for

the detection of non-active  $\text{Cs}^+$ , i.e. the use of a  $\text{K}^+$  saturated ion exchange (IX) barrier located immediately adjacent to the concrete on the cathodic side of the phantom. The IX barrier, containing saturated  $\text{K}^+$  form resin, provides a radiological titration to determine the flux of migrating non-active  $\text{Cs}^+$  ions; migrating  $\text{Cs}^+$  ions enter the IX resin and displace  $\text{K}^+$  ions from the matrix which then enter the catholyte for counting.

This radiological titration, though allowing for the detection of a non-active substance, has an additional experimental uncertainty than that exhibited for direct measurement of electrokinetically transported ions as per the  $\text{K}^+$  transport study. The propagation of these two errors through to the final calculation of ionic flux and simplified-Nernst-Planck diffusion coefficient values results in the CoV values reported for this system. As stated above, the final magnitude of the uncertainty associated with this method essentially renders accurate quantitative comparison difficult. However, this is the first description of such a radiological titration technique in literature and, as such, is still in its infancy. It has shown clear evidence for the flux of  $\text{Cs}^+$ , solely based on the detection of displaced potassium ions from the IX matrix. It therefore has significant potential as a bench-top method for teaching and nuclear decommissioning technique development.

## **Conclusion**

This study has demonstrated the possibility of detecting the transport of non-active caesium using radiometric methods without the hazards normally associated with laboratory study of radioactive caesium. Though further development of the ion exchange barrier and detection regime are needed to reduce the experimental error, the results indicate that such techniques could be invaluable in proof-of-concept studies necessary for the development of future decommissioning technologies.

## Acknowledgements

This work was funded by the United Kingdom's Nuclear Decommissioning Authority (NDA) through a PhD bursary for Andrew Parker. Colin Boxall is supported by the Lloyd's Register Foundation, an independent charity that supports the advancement of engineering related education, and funds research and development that enhances the safety of life at sea, on land, and in the air.

## References

- [1] A. J. Parker, C. Boxall, and M. J. Joyce, "A method for the replacement of  $^{137}\text{Cs}$  with  $^{40}\text{K}$  as a non-hazardous radioactive tracer for open-source decommissioning research applications," *J. Radioanal. Nucl. Chem.*, vol. 295, no. 2, pp. 797–802, Feb. 2013.
- [2] A. J. Parker, M. J. Joyce, and C. Boxall, "A radioanalytical phantom for assessing the efficacy of electrokinetic decontamination of entrained radioactivity within concrete media," *J. Radioanal. Nucl. Chem.*, vol. 300, no. 2, pp. 769–777, Feb. 2014.
- [3] Lanxess and Lewatit, "Lewatit MonoPlus S 108 KR," *Product Information Lewatit Ion Exchange Resins*, 2011. [Online]. Available: [http://www.lewatit.com/ion/en/products/ion\\_result.php](http://www.lewatit.com/ion/en/products/ion_result.php).
- [4] A. J. Parker, C. Boxall, M. J. Joyce, and P. Schotanus, "A thalium-doped sodium iodide well counter for radioactive tracer applications with naturally-abundant  $^{40}\text{K}$ ," *Nucl. Instruments Methods Phys. Res. Sect. A Accel. Spectrometers, Detect. Assoc. Equip.*, vol. 722, pp. 5–10, Sep. 2013.
- [5] C. Andrade, "Calculation of Chloride Diffusion Coefficients in Concrete From Ionic Migration Measurements," *Cem. Concr. Res.*, vol. 23, pp. 724–742, 1993.
- [6] C. Andrade, M. Castellote, C. Alonso, and C. Gonz, "Non-steady-state chloride diffusion coefficients obtained from migration and natural diffusion tests . Part I : Comparison between several methods of calculation," vol. 33, pp. 21–28, 2000.
- [7] M. Castellote, C. Andrade, and C. Alonso, "Measurement of the steady and non-steady-state chloride diffusion coefficients in a migration test by means of monitoring the conductivity in the anolyte chamber Comparison with natural diffusion tests," *Cem. Concr. Res.*, vol. 31, pp. 1411–1420, 2001.

- [8] F. Frizon, S. Lorente, and C. Auzuech, “Nuclear decontamination of cementitious materials by electrokinetics: An experimental study,” *Cem. Concr. Res.*, vol. 35, no. 10, pp. 2018–2025, Oct. 2005.
- [9] M. Castellote, C. Andrade, and C. Alonso, “Application of Electrical Fields in the Study of Concretes with respect to the Transport of Several Ionic Species Present in Radioactive Wastes : Characterisation and Decontamination .,” no. August, 2001.
- [10] P. Bevington and D. K. Robinson, *Data Reduction and Error Analysis for the Physical Sciences*, 3rd ed. McGraw-Hill, 2003.